IEEE Access
Multidisciplinary | Rapid Review | Open Access Journal

Received March 18, 2020, accepted April 7, 2020, date of publication April 21, 2020, date of current version May 8, 2020.

Digital Object Identifier 10.1109/ACCESS.2020.2989141

New Equivalent model and Modal Analysis of Stator Core-Winding System of Permanent Magnet Motor With Concentrated Winding

HONGBIN YIN[1,2], XUEYI ZHANG[1], FANGWU MA[2], CANSONG GU[2,3], HUI GAO[3], AND YONGCHAO WANG[3]

[1]School of Transportation and Vehicle Engineering, Shandong University of Technology, Zibo 255000, China
[2]State Key Laboratory of Automotive Simulation and Control, Jilin University, Changchun 130000, China
[3]China Automotive Technology and Research Center Company, Ltd., Tianjin 300300, China

Corresponding author: Xueyi Zhang (zhangxueyi@sdut.edu.cn)

This work was supported in part by the National Natural Science Foundation of China under Grant 51875327 and in part by the Doctor Foundation of Shandong University of Technology under Grant 4041-419088.

ABSTRACT An accurate prediction of modal characteristics of motor stator is essential in order to design a low vibration motor and to operate it quietly. Scholars have done a lot of research on the modal analysis of stator core and winding. However, there are few papers for the 0th-order mode shape and frequency of the stator system. This paper aims to propose a new stator system analysis model, which can effectively analyze the 0th-order mode and improve the model calculation efficiency. Firstly, the modal of stator core and stator core-winding system were analyzed theoretically. Secondly, four stator system finite element analysis models were established. The modal analysis of the stator core and stator core-winding system were carried out using the four models. The validity and computational efficiency of the four models of the stator core and stator core-winding system were compared. A new stator system analysis model was proposed. Thirdly, the modal tests of the stator core and stator core-winding system were carried out by hammering method, and the validity of the finite element analysis model was verified. Compared with the traditional model, the newly proposed model can analyze the 0th-order mode more effectively and improve the computational efficiency.

INDEX TERMS New equivalent model, 0th-order mode, stator core, winding, modal analysis.

I. INTRODUCTION

As motor design is key to the development of electric vehicles (EVs) and hybrid EVs (HEVs), it has recently become the subject of considerable interest [1]–[3]. An accurate prediction of modal characteristics of motor stator is essential in order to design a low vibration motor and to operate it quietly [4], [5]. The modal analysis of the stator core and winding is a difficult point in motor modal analysis. Scholars have done a lot of research on the modal analysis of stator cores and windings.

Since the stator core is a typical laminate structure, its stiffness will increase without considering the stacking effect, and then the calculated natural mode frequency deviates greatly from the actual situation. It is not reasonable to use the material properties of silicon steel sheet directly in the modelling process of stator core. In paper [5], a method to identify the physical parameters of laminated core and windings is proposed based on the modal testing of the motor stators with different conditions. Comparing the results of 3-D finite element analysis and experimental measurements, the equivalent Young's modulus of the isotropy laminated stator core and the windings are obtained. The stator is treated as homogeneous orthotropic laminate structure material, the recommended fitting curve is used to obtain material property parameters [6]. In paper [7], the laminated stator core is assumed to be modeled as a continuous solid with composite material, of which the equivalent Young's modulus is calculated by the Voigt–Reuss formula. In addition, since the circumferential modes have a major contribution in vibration generation, the equivalent material properties assigned to the stator core are isotropic. In paper [8], a novel approach of equivalent material identification is developed for multi-layered orthotropic structures. A numerical model of a laminated

The associate editor coordinating the review of this manuscript and approving it for publication was Zhong Wu.

stack's dynamics applicable to general laminated structures was developed. A simple linear contact model facilitated the computational efficiency and in this way enabled the modeling of the stack's dynamics using a large number of laminas [9]. Paper [10] introduces a simple and nondestructive method for the measurement of Young's modulus; it is then used in a finite-element (FE) program to determine the resonant frequencies of SRM (switched reluctance motor) stator vibration. The effects of mass density and Poisson's ratios are also discussed. The FE results are validated by vibration tests, which show good accuracy. The effects of laminated core on the rotor mode shapes are investigated in paper [11], experimental modal analysis was carried out for shaft and for rotor core mounted on shaft.

Paper [12] examines the effects of the stator windings and end-bells on stator modal vibration frequencies. The effect of the windings is equated to an increase of the pole mass. In paper [13], six kinds of winding equivalent models are established, and then compared with the modal test results. Taking a 48-slot 8-pole permanent magnet synchronous motor as an example, the influence of winding structure, winding immersion paint and winding end on the natural frequency of the stator of the motor is studied in paper [14]. Compared with the stator core structure, the natural frequencies of the low-order radial modes such as the 2nd, 3rd, and 4th steps of the core-and-winding structure are reduced before the varnishing, and the natural frequency is increased after the varnishing. The immersion process can greatly improve the structural rigidity and natural frequency of the motor. Comparing the calculated values with the measured values, the effect of the stator core shape and stiffness of windings in the slots are studied, as a result, in the 2.2kW motor, an equivalent Young's modulus as stiffness of windings in the slots is obtained as being about 1/100th that of copper [15]. In paper [16], the material properties of the orthotropic laminate structure and the windings were determined by finite element analysis and experimental measurements, and compared with the measured results. Studies have shown that for large asynchronous motors, the stator windings have a great influence on the natural frequency, and the elastic modulus is much lower than that of solid copper. The effective part of the winding and the end winding cannot simply calculate the natural frequency in the form of additional mass; the end winding quality and The effect of stiffness on the natural frequency generally cancels each other out, so the effect of the end winding on the natural frequency is relatively small. Paper [17] shows the development of a material model of the complete stator bar. Special attention was paid to the experimental determination of the material characteristics of the orthotropic composite space brackets. The numerical results have been evaluated against measurement.

In summary, scholars have done a lot of research on the modal analysis of stator core and winding. The research focuses on the analysis of the equivalent material properties of the stator core and winding, and the influence of the winding on the stator core mode. However, there are few papers for the 0th-order mode shape and frequency of the stator system. According to the existing literature, when the winding is equivalent to the model of additional mass, the 0th-order mode shape of the stator core shows good, but the contribution of the stiffness of the winding cannot be considered, and the deviation of the calculation result is large; when the winding is equivalent to a continuous entity, a large number of local modalities are generated, which reduces the efficiency of modal analysis.

This paper aims to propose a new stator system analysis model, which can effectively analyze the 0th-order mode, reduce the number of local modes caused by the stator winding equivalent model, and improve the model calculation efficiency. In section 2, the modal of stator core and stator core-winding system are analyzed theoretically and compared with the results of finite element analysis. The results show that the influence of winding on stator core is divided into additional mass and stiffness. The influence of stiffness is not ignore. In section 3, four stator system finite element analysis models are established. It is demonstrated that model 1 and model 3 are effective in paper [4]. In this paper, model 1 and model 3 are improved based on previous research results, model 2 and model 4 are obtained respectively. The modal analysis of the stator core and stator core-winding system is carried out using the four models. The validity and computational efficiency of the four-mode analysis of the stator core and stator core-winding system are compared. The influence of the winding on the stator core mode is analyzed by model 4.

In section 4, the modal tests of the stator core and stator core-winding system are carried out by hammering method, and the validity of the finite element analysis model is verified. In section 5, some conclusions are drawn.

II. THEORETICAL ANALYSIS

In the conventional method, the stator core-winding system is simplified to a ring having a certain thickness, and the stator teeth and windings are simplified to an additional mass. The natural frequency of the m-order mode in the circumferential direction of the stator system can be expressed as

$$f_m = \frac{1}{2\pi}\sqrt{\frac{K_m}{M_m}} \tag{1}$$

where K_m is the concentrated stiffness of the stator system (N/m), M_m is the concentrated mass of the stator core-winding system (kg).

The concentrated stiffness and concentrated mass of the 0th-order mode (also called the breathing mode) in the circumferential direction can be expressed by equations (2) and (3), respectively.

$$K_0 = 4\pi\frac{E_c h_c L_i}{D_c} \tag{2}$$

$$M_0 = M_c k_{md} = \pi D_c h_c L_i p_c k_i k_{md} \tag{3}$$

where, E_c is the Young's modulus, h_c is the thickness of the core, M_c is the mass, D_c is the average diameter, ρ_c is mass density of stator core, k_i is lamination coefficient, k_{md} is additional mass factor. The k_{md} can be expressed by the formula (4).

$$k_{md} = 1 + \frac{M_t + M_w + M_i}{M_c} \tag{4}$$

where, M_t is the mass of the stator teeth, M_w is the mass of the stator winding, M_i is the mass of the insulation.

Bringing the formulas (2) and (3) into the equation (1), the frequency of the 0th order mode in the circumferential direction is

$$f_0 = \frac{1}{\pi D_c}\sqrt{\frac{E_c}{\rho_c k_i k_{md}}} \tag{5}$$

Equation (5) shows that the natural frequency of the 0th-order mode is inversely proportional to the stator diameter, square root of density, lamination coefficient, and addition mass coefficient. This indicates that motors with smaller diameters, densities, lamination factors, and addition mass coefficient have higher frequencies. The natural frequency of the 0th order mode is proportional to the square root of Young's modulus. This indicates that the motor with higher elastic modulus has a higher 0-order mode natural frequency.

The natural frequency of the mth mode ($m \geq 2$) can be expressed as

$$f_m = f_0 \frac{m(\mathrm{m}^2 - 1)}{\sqrt{m^2 + 1}} k_a F_m \tag{6}$$

where,

$$F_m = \left\{1 + \frac{\kappa^2(\mathrm{m}^2 - 1)\left[m^2(4 + k_{mrot}/k_{md}) + 3\right]}{m^2 + 1}\right\}^{-1/2} \tag{7}$$

$$\kappa = \frac{h_c}{\sqrt{3}D_c} \tag{8}$$

$$k_{mrot} = 1 + \frac{s_1 c_t L_i h_t^2}{\pi D_c I_c}\left(1 + \frac{M_w + M_i}{M_t}\right)(4\mathrm{h}_t^2 + 6\mathrm{h}_c\mathrm{h}_t + 3\mathrm{h}_c^2) \tag{9}$$

In Equation (9), k_{mrot} is the additional mass factor for rotation, s_1 is the number of stator teeth (slots), c_t is the tooth width, and h_t is the tooth height, I_c is the area moment of inertia about the neutral axis parallel to the cylinder axis.

$$I_c = \frac{h_c^3 L_i}{12} \tag{10}$$

Taking a 2.2kW concentrated winding permanent magnet brushless DC motor for electric vehicle as an example, the modal of the stator core-winding system is calculated according to equation (5) and equation (6). The basic dimensions of the permanent magnet brushless DC motor are shown in Table 1, lamination coefficient $k_\mathrm{i} = 0.96$, Young's modulus $E_\mathrm{c} = 185000$MPa, mass density of stator core $\rho_\mathrm{c} = 7495$kg/m3, mass density of winding $\rho_\mathrm{cw} = 8960$kg/m3. The modal calculation results are shown in Table 2. The modal shape (m, n) represents the state of the stator system after deformation, m represents the order of the circumferential deformation, and n represents the order of the axial deformation.

TABLE 1. Basic dimensions of 10-pole 15-slot permanent magnet brushless DC motor.

Quantity	Unit	Value
Stator outer diameter	mm	140
Stator inner diameter	mm	99.6
The number of stator teeth	/	15
The tooth width	mm	8
The tooth height	mm	12
Axial length of the stator	mm	77.5
Stator yoke height	mm	6
Rotor outer diameter	mm	98.6
Permanent magnet thickness	mm	3
Pole embrace	/	0.9
Permanent magnet code	/	N35H
Iron core code	/	50A1000
Winding	/	Concentrated winding
Coil turns (per slot per phase)	/	3

TABLE 2. Comparison of ANALYTICAL ANALYSIS with finite element analysis results of stator core-Winding system.

Mode shape	Analytical analysis result (Hz)	Finite element analysis result (Hz)	Error（%）
(2,0)	501	579	-13.5
(3,0)	1405	1550	-9.35
(4,0)	2659	2783	-4.5
(5,0)	4228	4115	2.7
(0,0)	7269	6934	4.8

According to the analysis results of Table 2, the maximum error between the analytical method and the finite element method is 13.5%. Large error is caused while the stator teeth and windings are simplified to an additional mass. The winding is located in slots which are separated by steel teeth. According to [19], the tooth-slot zone with the winding can be regarded as an additional ring internal to the stator core yoke. Thus, the natural frequency of the stator core with the winding will be

$$f \approx \frac{1}{2\pi}\sqrt{\frac{K_m^{(c)} + K_m^{(w)}}{M_c + M_w}} \tag{11}$$

In equation (11), the effects of the winding on the equivalent mass and equivalent stiffness of the stator core are simultaneously considered.

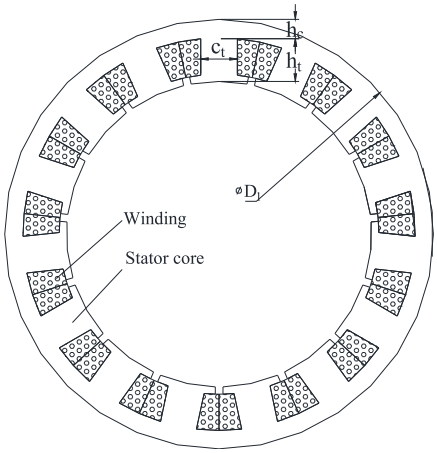

FIGURE 1. model of stator core-winding system.

III. MODELING AND MODAL ANALYSIS

A. EQUIVALENT model OF STATOR CORE

Accurately establishing the equivalent model of the stator core and defining the equivalent material properties of the stator core are the key to accurately analyzing the stator core mode. The stator core of the permanent magnet brushless DC motor is laminated by silicon steel sheets. In paper [4], the stator core is equivalent to the continuous entity composed of orthotropic materials, and the modal analysis is carried out by JMAG-Designer. The results are verified by experiment. In this paper, two kinds of model of the stator core are established.

(a) model 1: Stator core is equivalent to the continuous entity, the material type is set to orthotropy;
(a) model 2: Stator core is equivalent to the continuous entity, the material type is set to anisotropy.

The equivalent model of stator core is shown in Fig. 2. The equivalent material property settings for model 1 have been elucidated in [4]. In this paper, the equivalent material property settings for model 2 are explained.

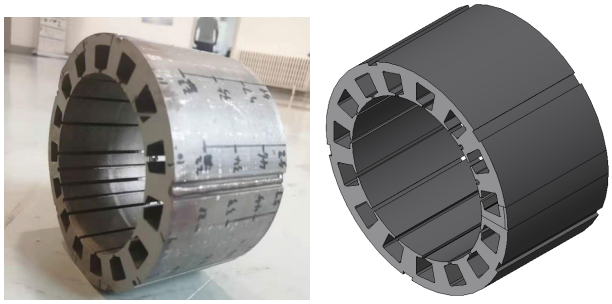

(a) Prototype (b) Equivalent model

FIGURE 2. Equivalent model of stator core.

Each components for the matrix displayed in the following formula should be specified when anisotropy is set according to paper [17].

$$\begin{Bmatrix} \sigma_x \\ \sigma_y \\ \sigma_z \\ \tau_{xy} \\ \tau_{yz} \\ \tau_{zx} \end{Bmatrix} = \begin{bmatrix} G_{11} & G_{12} & G_{13} & G_{14} & G_{15} & G_{16} \\ & G_{22} & G_{23} & G_{24} & G_{25} & G_{26} \\ & & G_{33} & G_{34} & G_{35} & G_{36} \\ & & & G_{44} & G_{45} & G_{46} \\ & & \text{symmetric} & & G_{55} & G_{56} \\ & & & & & G_{66} \end{bmatrix} \times \left[\begin{Bmatrix} \varepsilon_x \\ \varepsilon_y \\ \varepsilon_z \\ Y_{xy} \\ Y_{yz} \\ Y_{zx} \end{Bmatrix} - \begin{Bmatrix} A_x \\ A_y \\ A_z \\ A_{xy} \\ A_{yz} \\ A_{zx} \end{Bmatrix} (T - T_{\text{ref}}) \right] \quad (12)$$

where, $[\sigma]$ is stress, $[G_{ij}]$ is rigid matrix, $[\varepsilon]$ is strain, T is nodal temperature, T_{ref} is reference temperature, $[A]$ is thermal expansion vector, x, y, z, xy, yz, zx are components of the coordinate system applied to a material. Parameters are shown in table 3, the other parameters of rigid matrix are zero.

TABLE 3. The parameters of rigid matrix.

G_{11}	G_{22}	G_{33}	G_{44}	G_{55}	G_{66}
190000	190000	20000	100000	11300	11300

The calculation results of model 1 and model 2 are shown in table 4. The calculation error between model 1 and model 2 is within 1%, and the calculation accuracy is similar. model 1 cannot calculate the frequency of the (0,0)th order mode, and model 2 can calculate the frequency of the (0,0)th order mode.

TABLE 4. Comparison of analysis results of model 1 and model 2.

Mode shape	Analysis result of model 1 (Hz)	Analysis result of model 2 (Hz)	Error（%）
(2,0)	631	632	0.16
(2,1)	885	885	0
(3,0)	1703	1710	0.41
(3,1)	2155	2144	-0.51
(4,0)	3090	3102	0.39
(4,1)	3597	3578	-0.52
(5,0)	4616	4637	0.45
(5,1)	5186	5146	-0.77
(6,0)	6143	6165	0.36
(6,1)	6702	6691	-0.16
(0,0)	-	8236	-

B. EQUIVALENT model OF WINDING

As shown in Fig. 3(a), in the paper [4] the coil of stator winding is equivalent to a conductor that has the same shape as the stator slot and is in good contact with the stator slot. The analytical accuracy of this equivalent model is high. However, the model has many local modes of the winding,

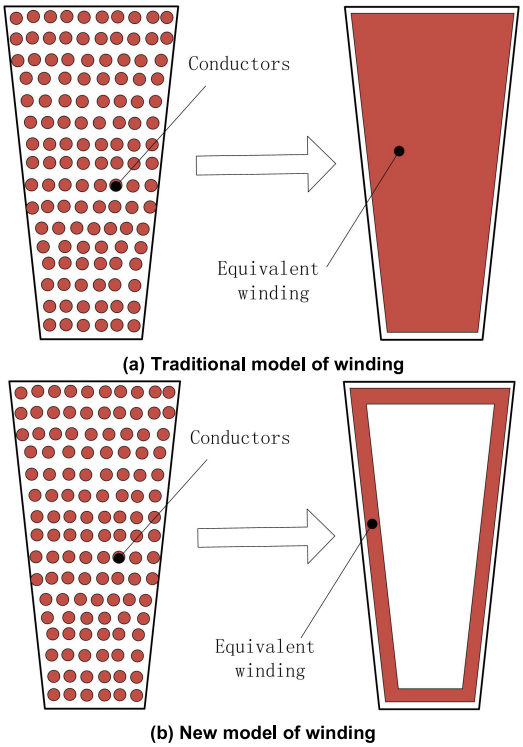

FIGURE 3. Equivalent model of winding.

which greatly reduces the calculation efficiency of modal analysis. At the same time, it is difficult to analyze the mode shape of the 0th-order mode because of the interference of a large number of local modes. To solve these problems, a new winding equivalent model is proposed. As shown in Fig. 3(b), the coil of stator winding is equivalent to a thin-walled tubular body that is in good contact with the stator slots. The thickness of the thin wall tube should be less than the length of the grid, in this paper, the thickness of the thin wall tube is 1.0 mm. As described in equation (11), the effect of this equivalent winding on the stator core mode has two aspects: (1) increase the equivalent mass of the stator core; (2) increase the equivalent stiffness of the stator core.

C. EQUIVALENT model OF STATOR CORE-WINDING SYSTEM

As shown in Fig. 4, based on the previously proposed models of the stator core and the winding, two models of the stator core-winding system are established.

(a) model 3: The stator core is equivalent to a continuous entity, and the material property is set to an anisotropic material; The windings are equivalent to mutually independent columnar bodies, the interface shape of the columnar body is consistent with the shape of the slot as shown in Fig.3(a), the material property is set to an orthotropic material.

(b) model 4: The stator core is equivalent to a continuous entity, and the material property is set to an anisotropic material; The windings are equivalent to thin-walled tubular bodies that is independent of each other, and the tubular body is closely connected to the stator slots, the material property is set to an orthotropic material.

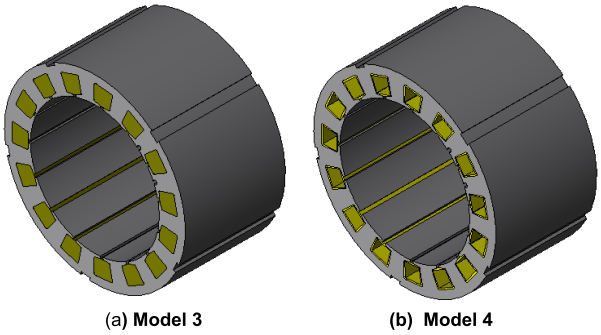

FIGURE 4. Equivalent model of stator core-winding system.

The material parameters of the stator core are shown in table 3, and the equivalent material parameters of the winding are shown in table 5.

TABLE 5. Equivalent material properties of winding.

Symbol	Unit	Model 3	Model 4
ρ	kg/m^3	5718	24000
E_x	MPa	135	500
E_z	MPa	200	300
ν_{xy}	-	0.3	0.3
ν_{yz}	-	0.1	0.1

The calculation results of model 3 and model 4 are shown in table 6. The analysis results show that the modal analysis results of the second to fifth orders are similar, and the error is controlled within 5%. model 3 cannot calculate the frequency of the (0,0)th order mode, and model 4 can calculate the frequency of the (0,0)th order mode.

TABLE 6. Comparison of analysis results of model 3 and model 4.

Mode shape	Analysis result of model 3 (Hz)	Analysis result of model 4 (Hz)	Error（%）
(2,0)	575	579	0.70
(2,1)	846	836	-1.18
(3,0)	1533	1550	1.11
(3,1)	1972	1972	0
(4,0)	2726	2783	2.09
(4,1)	3168	3214	1.45
(5,0)	3946	4115	4.28
(5,1)	4365	4551	4.26
(0,0)	-	6934	-

D. COMPARATIVE ANALYSIS OF 0TH ORDER MODE OF FINITE ELEMENT MODELS

The 0th-order mode has an important influence on the vibration noise of the permanent magnet motor for electric

vehicle driving according to paper [21], [22]. In this paper, the 0th-order mode of the stator core is analyzed based on model 1 and model 2. The analysis results are shown in Figure 5 and Figure 6.

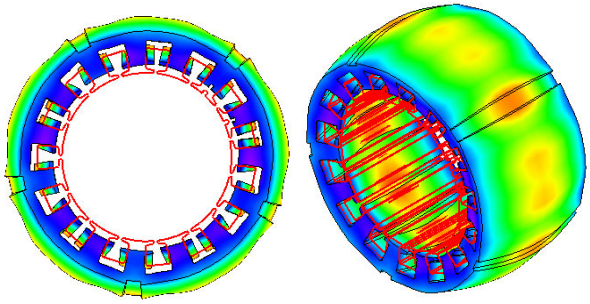

FIGURE 5. 0th-order mode of the stator core based on model 1.

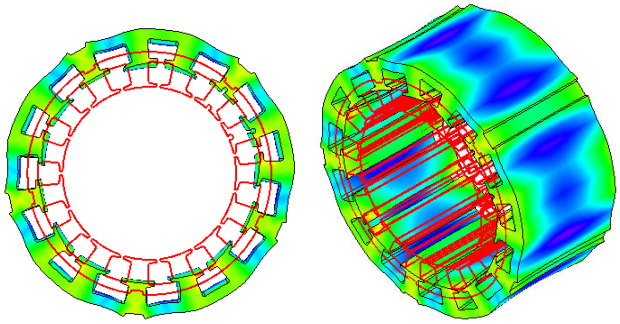

FIGURE 6. 0th-order mode of the stator core based on model 2.

It can be seen from the figure 5 that the 0th-order mode analyzed by model 1 is close to the (0, 2) order mode, and the mode shape of the (0, 0) order mode of the stator core cannot be well displayed. Based on the model 2, the (0, 0) order mode is well displayed as shown in the figure 6. In the commercial analysis software JMAG, the stator core equivalent material model has three types: isotropic material, orthotropic material and anisotropic material. When using an orthotropic material model, you need to input the equivalent Young's modulus in the three directions x, y, and z. If the equivalent Young's modulus in the z direction is too small, the 0-order modal shape is (0, 2) displayed as Figure5; when the anisotropic material model is used, the effect is improved, and the modal shape is (0, 0), as shown in Figure 6.

The analysis results of the 0th-order mode of the stator core-winding system analyzed based on the model 3 are shown in Fig. 7. It can be seen from the figure that the 0th-order mode of the stator system analyzed by the model 3 is approximated as the (0, 1) order mode shown as figure 7(a), and the stator winding has a very obvious local mode shown as figure7(b), which reduces the calculation efficiency. That because the winding uses orthotropic material model, the axial equivalent Young's modulus of the winding is too small.

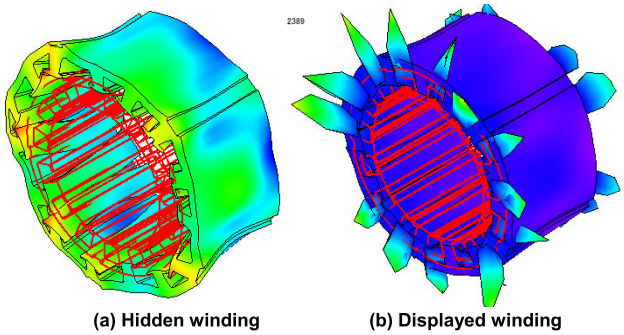

FIGURE 7. 0th-order mode of the stator core-winding system based on model 3.

The analysis results of the 0th-order mode of the stator core-winding system based on the model 4 are shown in Fig. 8. As can be seen from the figure, the modal shape of the 0th-order mode analyzed by the model 4 is very ideal, and the winding has no local mode, That because the winding model is changed to a thin walled tube model, the axial equivalent Young's modulus increases, and the effect is improved, the modal shape is (0,0) as shown in figure 8(a). Which is beneficial to improve the calculation efficiency.

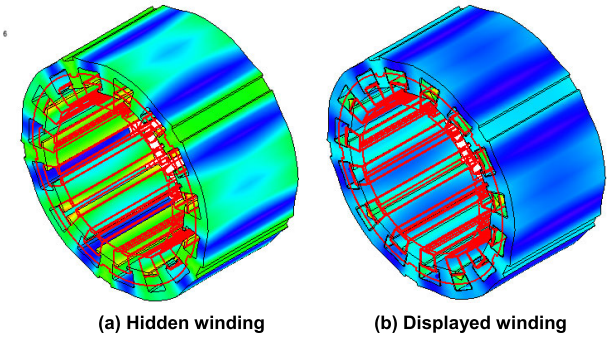

FIGURE 8. 0th-order mode of the stator core-winding system based on model 4.

E. COMPARATIVE ANALYSIS OF CALCULATION EFFICIENCY OF FINITE ELEMENT MODELS

In order to verify the computational efficiency of Model 1, model 2, model 3 and Model 4, the modal of the stator core-winding system is analyzed using the same computer. The CPU of the computer is Inter(R) Core(TM) i7-4810MQ, the memory capacity is 16GB, and the hard disk model is faspeed K5-256G SCSI.

When using model 1 for analysis, the analysis frequency range is 200∼8184Hz, which takes 46 seconds. When using model 2 for analysis, the analysis frequency range is 200∼8236Hz, and the consumption time is 39 seconds. The calculation speed of model 2 is higher than that of model 1 for using material type anisotropy instead of orthotropy.

When using model 3 for analysis, the analysis frequency range is 200∼8530Hz, which takes 29 minutes and 49 seconds. When using model 4 for analysis, the analysis

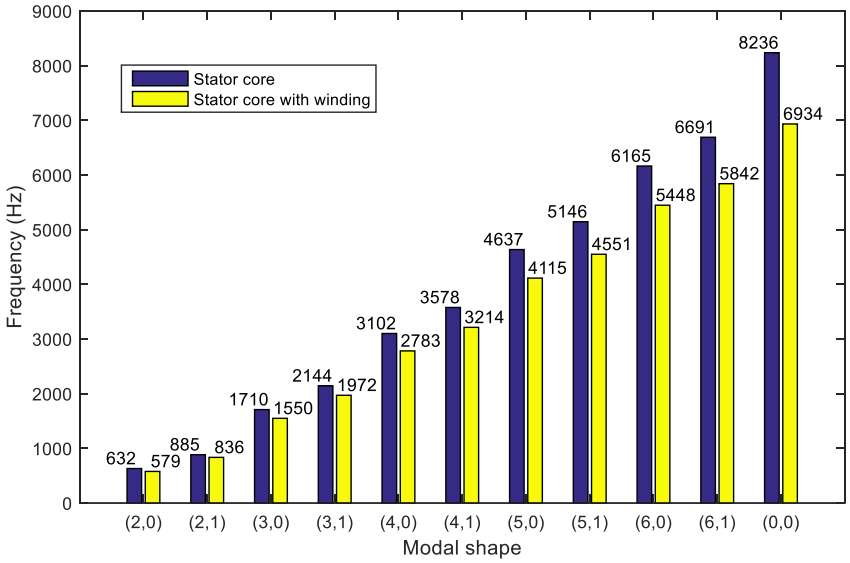

FIGURE 9. Influence of winding on stator core modal.

frequency range is 200∼9039Hz, and the consumption time is 12 minutes and 28 seconds. The calculation speed of model 4 is significantly higher than that of model 3 because the winding model in model 3 produces a large number of local modalities.

F. INFLUENCE OF WINDING ON MODAL OF STATOR CORE

The comparison results between the stator core and the stator core-winding system modality are shown in Fig. 9. It can be seen from the figure that the modal frequency of the stator core is reduced after considering the winding. The frequency of (0,0) mode is reduced from 8236Hz to 6934Hz, which is reduced by 1302Hz. Therefore, when the motor power is constant, it is important to improve the stiffness of the winding and reduce the winding quality to increase the frequency of the 0th-order mode of the motor.

IV. EXPERIMENT

A. MODAL TEST AND ANALYSIS OF STATOR CORE

In order to verify the validity of the finite element analysis, the modal tests of the stator core were carried out by the moving force hammer method. The test arrangement is shown in Figure 10. The test uses a 48-channel LMS-SCL220 data acquisition system, a PCB-356A33 acceleration sensor (frequency bandwidth 5120Hz), and 60 measurement points (5 rows in the circumferential direction and 12 columns in the axial direction) evenly arranged on the outer surface of the stator core. The test results are shown in Figure 11.

The peak of the frequency response curve in Fig. 11 is the natural frequency of each mode of the stator core. In the experimental test results, the modal order of the stator core includes (2, 0), (2, 1), (3, 0), (3, 1), (4, 0), (4,1) and (5, 0). The same order can be obtained by model analysis. Due to the accuracy of the sensor, the order (5, 1), (6, 0), (0, 0) obtained

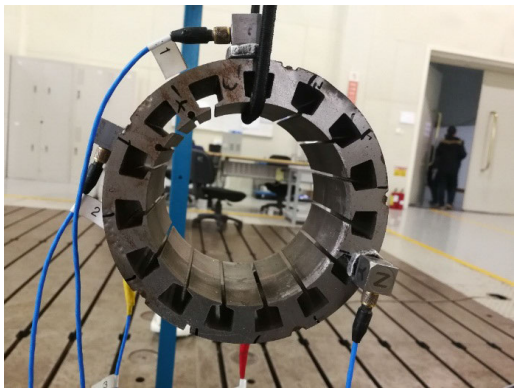

FIGURE 10. Modal test of stator core.

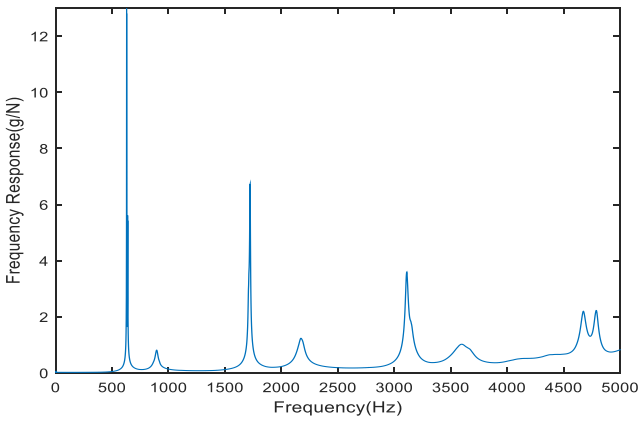

FIGURE 11. Frequency response of stator core experiment.

in the model cannot be obtained through experiments. However, we usually think that the obtained order comparison can verify the correctness of the model. In order to verify

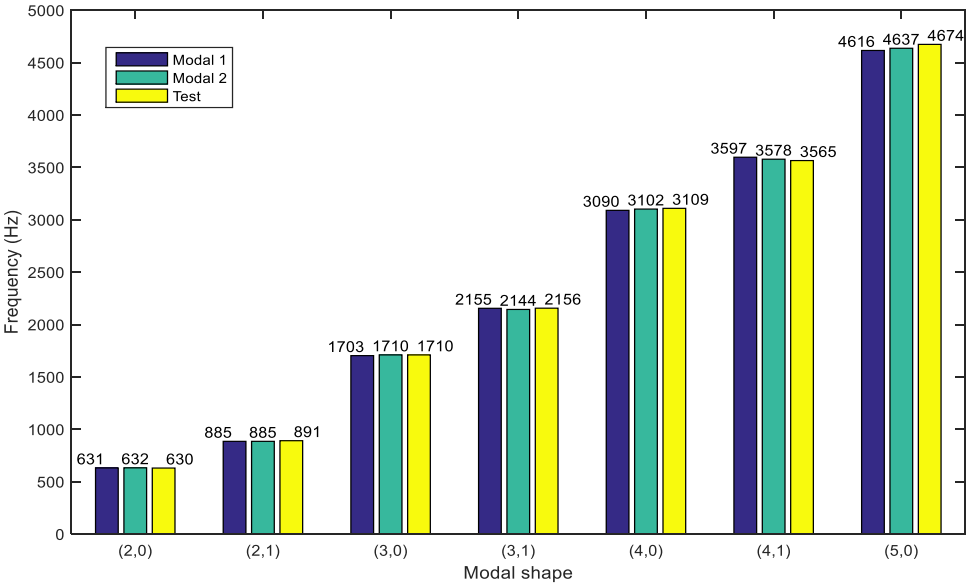

(a) Comparison of the results between FEA and experiment

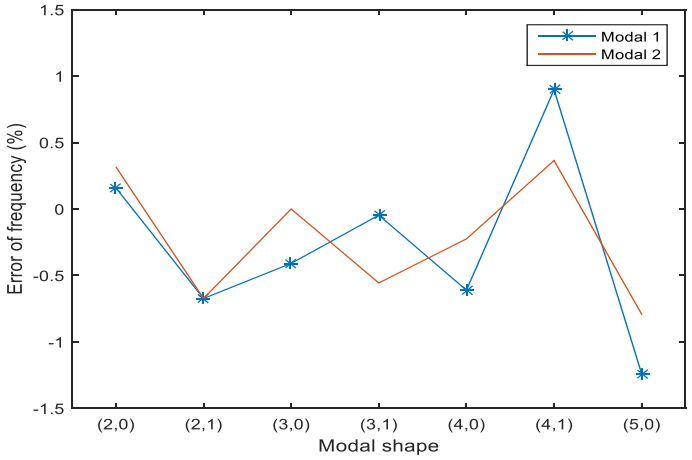

(b) Error of results between FEA and experiment

FIGURE 12. Comparative analysis of results between FEA and experiment of stator core.

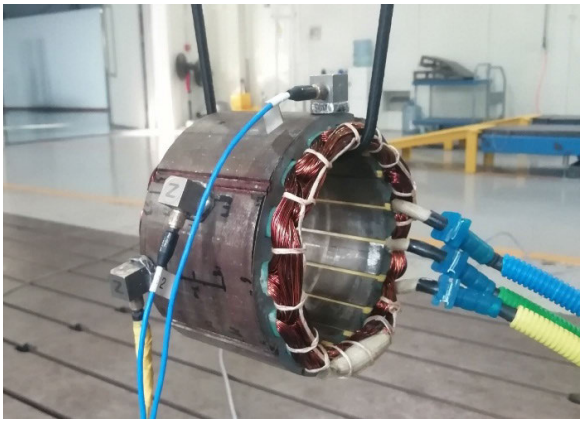

FIGURE 13. Modal test analysis of stator core with winding.

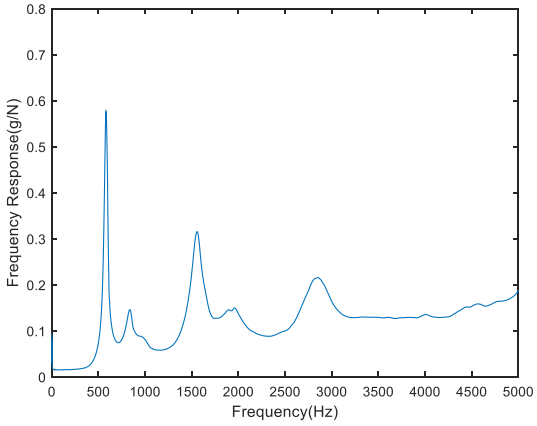

FIGURE 14. Modal experiment result of stator core with winding.

the correctness of the finite element model, the results of the experimental natural frequencies are compared with the finite element analysis results of model 1 and model 2.

The comparison results are shown in Figure 12. It can be seen from Fig. 12(a) that the absolute error of the finite element analysis results of the model 1, the model 2 and the

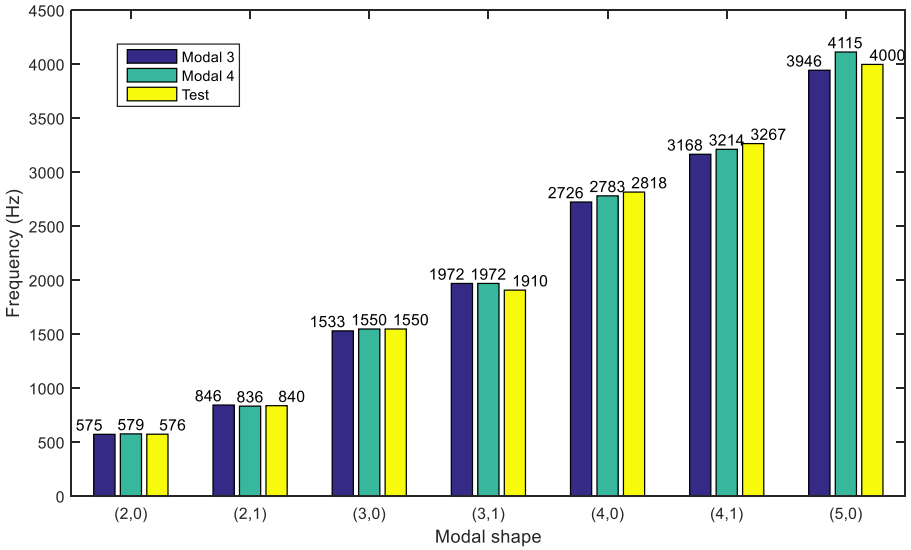

(a) Comparison of the results between FEA and experiment

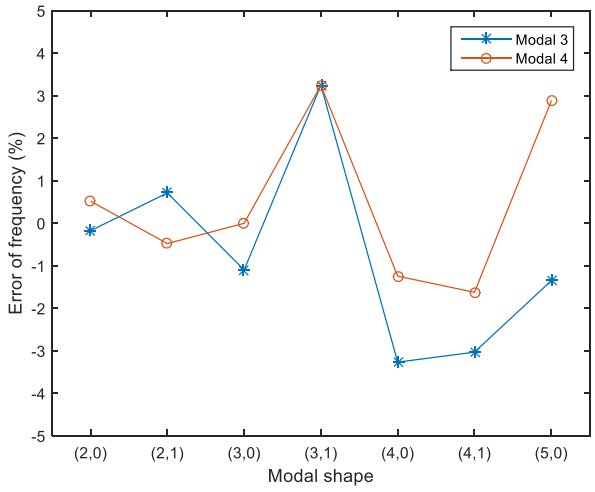

(b) Error of results between FEA and experiment

FIGURE 15. Comparative analysis of results between FEA and experiment of stator core.

modal test analysis results are small. It can be seen from Fig. 12(b) that the relative errors of Model 1, model 2 and the experimental analysis results are all controlled within 1.5%, the calculation accuracy is high. model 2 has higher accuracy than model 1.

B. MODAL TEST AND ANALYSIS OF STATOR CORE-WINDING SYSTEM

In order to verify the validity of the model 3 and model 4, the modal test of the stator core-winding system is carried out. The test method is the mobile hammer method, and the test sensor arrangement is shown in Figure 13. The test uses a 48-channel LMS-SCL220 data acquisition system, a PCB-356A33 acceleration sensor (frequency bandwidth 5120Hz), and 60 measurement points (5 rows in the circumferential direction and 12 columns in the axial direction) evenly arranged on the outer surface of the stator core.

The test results of stator core with winding are shown in Figure 14. The peak of the frequency response curve in Fig. 13 is the natural frequency of each mode. In the experimental test results, the modal order of the stator core includes (2, 0), (2, 1), (3, 0), (3, 1), (4, 0), (4,1) and (5, 0). The same order can be obtained by model analysis. Due to the accuracy of the sensor, the order (5, 1), (6, 0), (0, 0) obtained in the model cannot be obtained through experiments. However, we usually think that the obtained order comparison can verify the correctness of the model.A comparison of the test results with the finite element results is shown in Fig. 15. It can be seen from Fig. 15(a) that the absolute error between the analysis results of model 3 and model 4 and the experimental results is small. From Figure 15(b), it can be seen that the relative errors are all controlled within 4%. The maximum absolute error value of model 3 is 3.26%, and the maximum absolute error value of model 4 is 3.24%. model 4 not only improves the calculation efficiency, but also improves the calculation accuracy.

The comparison of analytical analysis and experiment is shown in table 7. It can be seen from the table that the

TABLE 7. Error analysis of analytical analysis method and finite element analysis method.

Mode shape	Test	Analytical analysis result (Hz)	Error of Analytical analysis result	Finite element analysis result (Model 4) (Hz)	Error of Finite element analysis result
(2,0)	576	501	-13%	579	0.5%
(3,0)	1550	1405	-9%	1550	0
(4,0)	2818	2659	-5.6%	2783	-1.2%
(5,0)	4000	4228	5.7%	4115	2.8%

maximum value of the absolute value of the analytical analysis is 13%, and the analysis accuracy is poor. The maximum value of the absolute value of the finite element model error is 2.8%, and the accuracy is high. The analytical analysis and calculation speed is fast, suitable for rapid calculation in the early design period, but accurate analysis is suitable for the final check and optimization of the model.

V. CONCLUSION

This paper aims to propose a new stator system analysis model. Firstly, the modal of stator core and stator core-winding system were analyzed theoretically. Secondly, four stator system finite element analysis models were established. The modal analysis of the stator core and stator core-winding system were carried out using the four models. The validity and computational efficiency of the four-mode analysis of the stator core and stator core-winding system were compared. Thirdly, the modal tests of the stator core and stator core-winding system were carried out by hammering method, and the validity of the finite element analysis model was verified. Some conclusions are drawn:

(1) The influences of winding on stator core are divided into additional mass and stiffness. When ignoring the equivalent stiffness of the winding, the modal analysis of the stator system produces a large error;

(2) A new stator system analysis model is proposed. As described in model 4, the stator core is equivalent to a continuous entity, and the material property is set to an anisotropic material; The winding is equivalent to thin-walled tubular bodies that are independent of each other, and the tubular body is closely connected to the stator slots;

(3) Compared with the traditional model, the newly proposed model can analyze the 0th-order mode more effectively;

(4) The newly proposed model can effectively reduce the local modal interference of winding and improve the computational efficiency.

ACKNOWLEDGMENT

Authors' special thanks go to Hongli Zhang, Peng Zhao, Lulu Wei, and Zeyu Zhang for their support and the fruitful technical discussions.

REFERENCES

[1] C. Hu, X. Tang, L. Zou, K. Yang, Y. Li, and L. Zheng, "Numerical and experimental investigations of noise and vibration characteristics for a dual-motor hybrid electric vehicle," *IEEE Access*, vol. 7, pp. 77052–77062, 2019.

[2] F. Ma, H. Yin, L. Wei, G. Tian, and H. Gao, "Design and optimization of IPM motor considering flux weakening capability and vibration for electric vehicle applications," *Sustainability*, vol. 10, no. 5, p. 1533, 2018.

[3] F. Ma, H. Yin, L. Wei, L. Wu, and C. Gu, "Analytical calculation of armature reaction field of the interior permanent magnet motor," *Energies*, vol. 11, no. 9, p. 2375, 2018.

[4] H. Yin, F. Ma, X. Zhang, C. Gu, H. Gao, and Y. Wang, "Research on equivalent material properties and modal analysis method of stator system of permanent magnet motor with concentrated winding," *IEEE Access*, vol. 7, pp. 64592–64602, 2019.

[5] J. Sun, H. Feng, and C. Zhu, "Identification of laminated core and winding's physical parameters by stator's modal testings," in *Proc. 17th Int. Conf. Electr. Mach. Syst. (ICEMS)*, Oct. 2014, pp. 1488–1492.

[6] Y.-H. Chen, T.-H. Ding, and L. Tian, "Research on calculation method of motor lamination core vibration characteristics," *Electr. Mach. Control*, vol. 18, no. 1, pp. 71–76, Jan. 2014.

[7] F. Chai, Y. Li, Y. Pei, and Z. Li, "Accurate modelling and modal analysis of stator system in permanent magnet synchronous motor with concentrated winding for vibration prediction," *IET Electr. Power Appl.*, vol. 12, no. 8, pp. 1225–1232, Sep. 2018.

[8] P. Millithaler, É. Sadoulet-Reboul, M. Ouisse, J.-B. Dupont, and N. Bouhaddi, "Structural dynamics of electric machine stators: Modelling guidelines and identification of three-dimensional equivalent material properties for multi-layered orthotropic laminates," *J. Sound Vibrat.*, vol. 348, pp. 185–205, Jul. 2015.

[9] M. Pirnat, G. Čepon, and M. Boltežar, "Introduction of the linear contact model in the dynamic model of laminated structure dynamics: An experimental and numerical identification," *Mechanism Mach. Theory*, vol. 64, pp. 144–154, Jun. 2013.

[10] Z. Tang, P. Pillay, A. M. Omekanda, C. Li, and C. Cetinkaya, "Young's modulus for laminated machine structures with particular reference to switched reluctance motor vibrations," *IEEE Trans. Ind. Appl.*, vol. 40, no. 3, pp. 748–754, May 2004.

[11] S. Singhal, K. V. Singh, and A. Hyder, "Effect of laminated core on rotor mode shape of large high speed induction motor," in *Proc. IEEE Int. Electr. Mach. Drives Conf. (IEMDC)*, May 2011, pp. 1557–1562.

[12] W. Cai, P. Pillay, and Z. Tang, "Impact of stator windings and end-bells on resonant frequencies and mode shapes of switched reluctance motors," *IEEE Trans. Ind. Appl.*, vol. 38, no. 4, pp. 1027–1036, Jul. 2002.

[13] R. Chen, S. Zuo, R. He, and L. He, "Stator FEM modeling of permanent magnet synchronous motor for electric vehicle driving based on structural vibration analysis," in *Proc. 2nd Int. Conf. Inf. Sci. Eng.*, Dec. 2010, pp. 5407–5411.

[14] L. Xiaohua, H. Surong, and Q. Zhang, "Analysis of natural frequencies of stator structure of permanent magnet synchronous motors for electric vehicles," *Proc. CSEE*, vol. 37, no. 8, pp. 2383–2390, 2017.

[15] S. Noda, S. Mori, K. Itomi, and F. Ishibashi, "Effect of coils on natural frequencies of stator cores in small induction motors," *IEEE Trans. Energy Convers.*, vol. EC-2, no. 1, pp. 93–99, Mar. 1987.

[16] T. Y. Wang and F. Wang, "Vibration and modal analysis of stator of large induction motors," *Zhongguo Dianji Gongcheng Xuebao(Proc. Chin. Soc. Electr. Eng.)*, vol. 27, no. 12, pp. 41–45, 2007.

[17] B. Schlegl, F. Schönleitner, F. Neumayer, F. Heitmeir, and A. Marn, "Analytical determination of the orthotropic material behavior of stator bars in the range of the end windings and determination of the material characteristics of the orthotropic composite space brackets via experimental modal analysis and FE-calculation," in *Proc. 12th Int. Conf. Elect. Mach.*, Sep. 2012, pp. 1948–1956.

[18] *JMAG-Designer 16.0. Help, Home, Functions of Analysis, Materials, Mechanical Properties*, JSOL, Tokyo, Japan, 2019.

[19] J. F. Gieras, C. Wang, and J. C. Lai, *Noise of Polyphase Electric Motors*. Boca Raton, FL, USA: CRC Press, 2018.

[20] M. Valavi, J. Le Besnerais, and A. Nysveen, "An investigation of zeroth-order radial magnetic forces in low-speed surface-mounted permanent magnet machines," *IEEE Trans. Magn.*, vol. 52, no. 8, pp. 1–6, Aug. 2016.
[21] G. Verez, G. Barakat, Y. Amara, and G. Hoblos, "Impact of pole and slot combination on vibrations and noise of electromagnetic origins in permanent magnet synchronous motors," *IEEE Trans. Magn.*, vol. 51, no. 3, pp. 1–4, Mar. 2015.

HONGBIN YIN was born in Shandong, China, in April 1986. He received the M.S. degree in power machinery and engineering from the Shandong University of Technology, Zibo, China, in 2012, and the Ph.D. degree from Jilin University, Changchun, China, in 2019.

Since 2015, he has been with the College of Automotive Engineering, Jilin University, Changchun, China, where he was involved in various research projects. He also worked for China Automotive Technology and Research Center Company, Ltd., as an Intern Engineer. Since 2019, he has been a Lecturer with the Shandong University of Technology. His research interests include control and modeling of electrical drives, design of electric machines, and the automotive applications of electric motor drives.

XUEYI ZHANG was born in 1963. He received the Ph.D. degree in mechanical and electronic engineering from the Shandong University of Science and Technology University, Qindao, China, in 2011. He is currently a Professor with the School of Transportation and Vehicle Engineering, Shandong University of Technology, China, a specially appointed expert of Taishan Scholars and a national candidate of Millions of Talents, who enjoys special allowances from the State Council Government. At present, he has 53 authorized patents, published 142 articles, and five monographs. His research interests include vehicle electrical and control technology, electric vehicle driving systems, and control technology. He received four items of the first prizes at provincial and ministerial level, and in 2006, he received the second prize for technological invention (ranking 1).

FANGWU MA received the B.S. and M.S. degrees in automotive engineering from Jilin University, Changchun, China, in 1982 and 1988, respectively, and the Ph.D. degree in mechanical engineering from Imperial College London, London, U.K., in 1999.

He was a Research Fellow on transportation design with Wolverhampton University, U.K. He was with Chrysler LLC as a Senior Engineer, taken charge of the vehicle research and development programs including Jeep Liberty, Dodge Ram, Caravan, and so on. He was the Chief Engineer and the Vice President of the Geely Research and Development Centre, in charge of developing GC7, GX7 and GX9, and the negotiation and recruitment training of IP and DDR during Geely Auto's Acquisition of Volvo. He is currently a "National Thousand Talents Plan" Distinguished Professor with Jilin University, China, and also the Executive Dean of the Qingdao Automotive Research Institute, Jilin University. He has published numerous technical articles, reviewed technical articles for SAE and other journals to enhance quality of publication, and invented patents related to automotive engineering. Further, he has actively participated, organized and contributed to many automotive related important conferences, e.g., SAE World Congress, Automotive Design Conference in Interior Motive, International Forum on Chinese Automobile Recycling, FISITA World Automotive Congress and Exhibition, International Conference on Globalization of Development and Innovation, International AVL Conference on Engine and Environment, JSAE Annual Spring Congress, and International Conference on NVH Technology. He also serves as an Editor-in-Chief for *Automotive Innovation*—an international journal on Automotive Engineering.

CANSONG GU received the B.S. degree in mechanical engineering from the Hebei University of Engineering, in 2004, and the M.S. degree in mechanical engineering from the Shijiazhuang Railway Institute, in 2007. He is currently pursuing the Ph.D. degree in automotive engineering with Jilin University, China.

Since 2007, he has been an Engineer with the China Automotive Technology and Research Center Company, Ltd. His research interests include the noise vibration and harshness (NVH) development of combustion engine, the vehicle NVH refinement and development using CAE analysis and prototype testing methods. Hi awards and honors the Deputy Secretary of the NVH Committee of China-SAE.

HUI GAO received the M.S. degree in mechanical engineering from the Hebei University of Technology, Tianjin, China, in 2010. He has been working on the infrastructure and application of drivetrain NVH facilities, including engine, hybrid drivetrain, and electric power systems, and is engaged in the research of NVH testing and evaluation techniques of the above systems, and their NVH development. He was also invited to host and participate in three national automotive industry standards for noise measurement in transmissions and electric drive systems.

YONGCHAO WANG received the B.S. degree vehicle engineering from Agricultural University of Hebei, in 2013, and the M.S. degree in mechanical engineering from the Hebei University of Technology, in 2016.

Since 2016, he has been a NVH Test Engineer with China Automotive Technology and Research Center Company, Ltd. (CATARC), Tianjin, China. His researches focus on NVH for automotive new energy motor and transmission.